# Therapeutic Efficacy of Potent Neutralizing HIV-1-Specific Monoclonal Antibodies in SHIV-Infected Rhesus Monkeys

Published in final edited form as:
*Nature*. 2013 November 14; 503(7475): 224–228. doi:10.1038/nature12744.

# Therapeutic Efficacy of Potent Neutralizing HIV-1-Specific Monoclonal Antibodies in SHIV-Infected Rhesus Monkeys

**Dan H. Barouch**[1,2,*], **James B. Whitney**[1], **Brian Moldt**[3], **Florian Klein**[4], **Thiago Y. Oliveira**[4], **Jinyan Liu**[1], **Kathryn E. Stephenson**[1], **Hui-Wen Chang**[1], **Karthik Shekhar**[5], **Sanjana Gupta**[5], **Joseph P. Nkolola**[1], **Michael S. Seaman**[1], **Kaitlin M. Smith**[1], **Erica N. Borducchi**[1], **Crystal Cabral**[1], **Jeffrey Y. Smith**[1], **Stephen Blackmore**[1], **Srisowmya Sanisetty**[1], **James R. Perry**[1], **Matthew Beck**[6], **Mark G. Lewis**[7], **William Rinaldi**[8], **Arup K. Chakraborty**[2,5], **Pascal Poignard**[3], **Michel C. Nussenzweig**[4,9,**], and **Dennis R. Burton**[2,3,**]

[1]Center for Virology and Vaccine Research, Beth Israel Deaconess Medical Center, Harvard Medical School, Boston, MA 02215, USA

[2]Ragon Institute of MGH, MIT, and Harvard, Cambridge, MA 02139, USA

[3]The Scripps Research Institute, La Jolla, CA 92037, USA

[4]The Rockefeller University, New York, NY 10065, USA

[5]Massachusetts Institute of Technology, Cambridge, MA 02139, USA

[6]New England Primate Research Center, Southborough, MA 01776, USA

[7]Bioqual, Inc., Rockville, MD, USA

[8]Alpha Genesis, Inc., Yemassee, SC 29945, USA

[9]Howard Hughes Medical Institute, USA

## Abstract

HIV-1-specific monoclonal antibodies (mAbs) with extraordinary potency and breadth have recently been described. In humanized mice, combinations of mAbs have been shown to suppress viremia, but the therapeutic potential of these mAbs has not yet been evaluated in primates with an intact immune system. Here we show that administration of a cocktail of HIV-1-specific mAbs, as well as the single glycan-dependent mAb PGT121, resulted in a rapid and precipitous decline of plasma viremia to undetectable levels in rhesus monkeys chronically infected with the pathogenic virus SHIV-SF162P3. A single mAb infusion afforded up to a 3.1 log decline of plasma viral RNA in 7 days and also reduced proviral DNA in peripheral blood, gastrointestinal mucosa, and

*Correspondence should be addressed to: D.H.B. (dbarouch@bidmc.harvard.edu).
**These authors contributed equally

**Author Contributions**

D.H.B., M.C.N., and D.R.B. designed the studies. J.B.W., B.M., F.K., T.Y.O., H.W.C., S.S., and P.P. led the virologic assays. B.M., J.L., K.E.S., M.S.S., K.M.S., E.N.B., C.C., J.Y.S., S.B., and J.R.P. led the immunologic assays. K.S., S.G., and A.K.C. led the kinetic analyses. J.B.W., J.P.N., M.B., M.G.L., and W.R. led the mAb infusions and clinical care of the rhesus monkeys. D.H.B. led the studies and wrote the paper with all co-authors.

The authors declare no competing financial interests. M.C.N. and D.R.B. are co-inventors on patents covering the mAbs utilized in the present study.

lymph nodes without the development of viral resistance. Moreover, following mAb administration, host Gag-specific T lymphocyte responses exhibited improved functionality. Virus rebounded in the majority of animals after a median of 56 days when serum mAb titers had declined to undetectable levels, although a subset of animals maintained long-term virologic control in the absence of further mAb infusions. These data demonstrate a profound therapeutic effect of potent neutralizing HIV-1-specific mAbs in SHIV-infected rhesus monkeys as well as an impact on host immune responses. Our findings strongly encourage the investigation of mAb therapy for HIV-1 in humans.

A series of broad and potent HIV-1 Env-specific mAbs have recently been isolated[1,2] and have been shown to target the CD4 binding site[3–7], the V1/V2 loops[8,9], the V3/V4 loops and N332 glycans[10–13], and the membrane proximal external region (MPER)[14]. Previous studies in humanized mice and humans using the earlier generation of HIV-1 Env-specific mAbs suggested that the therapeutic potential of mAbs would be severely limited by the rapid emergence of viral escape mutations in the context of diverse virus swarms[15–17]. However, cocktails of 3 or 5 of the new generation of more potent mAbs targeting multiple epitopes have recently been shown to suppress HIV-1 replication in humanized mice[18,19].

## Therapeutic efficacy of mAb cocktails

To evaluate the therapeutic potential of broad and potent HIV-1-specific mAbs in primates with an intact immune system, we infused cocktails of mAbs, as well as single mAbs, into chronically SHIV-infected rhesus monkeys. We focused on the N332 glycan-dependent mAb PGT121[10] and the CD4 binding site-specific mAbs 3BNC117[6] and b12[20]. In the first study, we utilized 8 Indian origin adult rhesus monkeys (*Macaca mulatta*) that did not express the class I alleles *Mamu-A*01*, *Mamu-B*08*, and *Mamu-B*17* and that were infected intrarectally with the pathogenic virus SHIV-SF162P3 for 9 months before the mAb infusions. These animals exhibited chronic setpoint viral loads of 3.4–4.9 log RNA copies/ml with clinical disease progression and reduced CD4+ T lymphocyte counts. We performed two intravenous mAb infusions on day 0 and day 7 with 10 mg/kg of each of PGT121, 3BNC117, and b12 (N=4); or with 30 mg/kg of the isotype matched control mAb DEN3 (N=1) or saline (N=3).

Following the initial mAb infusion, we observed rapid and precipitous declines of plasma viral loads to undetectable levels by day 7 in 4 of 4 monkeys (Fig. 1a). Virologic control persisted for 84 to 98 days in animals 82-09, 98-09, and 161-09 (Fig. 1b). Following viral rebound, sequence analysis[18,21] showed no N332 or other characteristic escape mutations (Supplementary Information), and rebound correlated with the decline of serum mAb titers to undetectable levels <1 μg/ml (Extended Data Fig. 1). Monkey 82-09 exhibited transient viremia on day 28 (Fig. 1b), which correlated with the decline of serum mAb titers to undetectable levels (Extended Data Fig. 1), but this animal then spontaneously re-controlled viral replication until day 98. Monkey 163-09, which had the lowest baseline viral load of 3.4 log RNA copies/ml prior to the mAb infusion, exhibited long-term virologic control for over 200 days despite the absence of detectable serum mAb titers after day 70 (Fig. 1b). Proviral DNA in PBMC also declined rapidly by 10-fold in the monkeys that received the mAbs (Fig. 1e). Virologic control was not observed in the monkeys that received DEN3 or

saline (Fig. 1c, d), and viral loads on day 14 were significantly lower in the mAb treated monkeys than in the controls (P=0.02, Mann-Whitney test).

As expected, serum neutralizing antibody (NAb) ID50 titers[22] to the SHIV-SF162P3 challenge virus increased dramatically following the mAb administration and then declined over time (Extended Data Fig. 2). Following clearance of the mAbs, NAb titers to SHIV-SF162P3 as well as to the related neutralization-sensitive virus SHIV-SF162P4 remained slightly higher than baseline titers (Extended Data Fig. 2). The magnitude of Gag-specific CD8+ and CD4+ T lymphocyte responses[23,24] was not detectably modulated following mAb administration (Extended Data Fig. 3), but by day 28, we observed 3- and 5-fold reductions, respectively, in the percentage of Gag-specific CD8+ and CD4+ T lymphocytes that expressed the exhaustion and activation markers PD-1 and Ki67 (Fig. 1g, h; P=0.02). Moreover, CD8+ T lymphocytes from these animals exhibited increased functional capacity to suppress virus replication following mAb administration[25] (Fig. 1f; P=0.03). These data suggest that mAb administration not only exerted direct antiviral effects but also improved host immune responses.

We next investigated the therapeutic efficacy of a single infusion of the cocktail of three mAbs as well as a combination of only two mAbs. 14 rhesus monkeys infected with SHIV-SF162P3 for 9 months prior to the mAb infusion with chronic setpoint viral loads of 3.2–5.6 log RNA copies/ml received a single infusion on day 0 with 10 mg/kg of each of the mAbs PGT121, 3BNC117, and b12 (N=5); PGT121 and 3BNC117 (N=5); or the isotype matched control mAb DEN3 (N=4). We observed rapid virologic control to undetectable levels by day 7 in 3 of 5 animals that received the cocktail of three mAbs and in 5 of 5 animals that received only PGT121 and 3BNC117 (Fig. 2a, b). The 2 animals that failed to achieve complete virologic suppression had the highest baseline plasma viral loads of 5.4 and 5.6 log RNA copies/ml before the mAb infusion and exhibited 2.8 and 2.9 log declines, respectively, in plasma viremia prior to rapid viral rebound on day 21 (monkeys 4907, 4909; Fig. 2a). No characteristic viral escape mutations were detected following viral rebound (Supplementary Information). The animals that suppressed viral loads to undetectable levels exhibited up to a 3.1 log decline of plasma viral RNA copies/ml by day 7 (monkey 4912; Fig. 2b). Viral rebound occurred in the majority of animals between day 28 and day 84 (Fig. 2a, b) and was associated with declines of serum mAb titers to undetectable levels (Extended Data Fig. 4). The animal with the lowest baseline viral load of 3.2 log RNA copies/ml exhibited long-term virologic control for over 100 days (monkey 4905; Fig. 2b), and viral loads on day 14 were significantly lower in both groups of mAb treated monkeys than in the controls (P=0.01). One control animal (monkey 5324; Fig. 2c) was euthanized for progressive clinical AIDS and opportunistic infections during the course of this experiment. PGT121 and 3BNC117 administration also resulted in 3- and 4-fold reductions in the percentage of PD-1+Ki67+ Gag-specific CD8+ and CD4+ T lymphocytes, respectively (Fig. 2e, f).

To confirm that viral rebound was not associated with the development of viral resistance to the mAbs, we performed a second infusion of mAbs on day 105 in the monkeys that received PGT121 and 3BNC117. Viral re-suppression was observed in 4 of 4 animals following the second mAb infusion (Fig. 2d; Supplementary Information). However,

virologic control appeared less durable and serum mAb titers were lower following the second mAb infusion as compared with the first mAb infusion (Fig. 2b, d; Extended Data Fig. 4), presumably as a result of monkey anti-human antibody responses that developed following the first mAb administration (Extended Data Fig. 5). Nevertheless, we assessed the impact of the second mAb infusion on proviral DNA in various tissue compartments[26,27] and observed a 2-fold decline in lymph nodes (P=0.1; Fig. 2g) and a 3-fold decline in gastrointestinal mucosa (P=0.02; Fig. 2h) 14 days following mAb re-administration. These data indicate that the potent mAbs not only suppressed viremia but also reduced proviral DNA in tissues without the generation of viral resistance.

## Therapeutic efficacy of single mAbs

Although the cloned SHIV-SF162P3 pseudovirus is highly sensitive to 3BNC117, we observed that our particular SHIV-SF162P3 challenge stock was largely resistant to 3BNC117 (Extended Data Fig. 6), which raised the possibility that the observed therapeutic efficacy in the previous experiment may have been due to PGT121 alone. We therefore performed a single infusion of 10 mg/kg PGT121 alone (N=4), 3BNC117 alone (N=4), or the control mAb DEN3 (N=4) in 12 rhesus monkeys infected with SHIV-SF162P3 for 9 months prior to the mAb infusion with chronic setpoint viral loads of 3.3–5.4 log RNA copies/ml. PGT121 alone resulted in rapid virologic control to undetectable levels by day 7 in 4 of 4 animals, followed by viral rebound by day 42 to day 56 in 3 animals that again correlated with declines in serum PGT121 titers to undetectable levels (Fig. 3a, c; Extended Data Fig. 7; P=0.02 comparing viral loads on day 14 in PGT121 treated animals compared with controls). One animal exhibited long-term virologic control (monkey DN1G; Fig. 3a). PGT121 alone also reduced proviral DNA by 6-fold in peripheral blood (P=0.05; Fig. 3d), 4-fold in lymph nodes (P=0.05; Fig. 3e), and 4-fold in gastrointestinal mucosa (P=0.1; Fig. 3f) as compared with the DEN3 control on day 14. Moreover, PGT121 alone resulted in 3- and 5-fold reductions in the percentage of PD-1+Ki67+ Gag-specific CD8+ and CD4+ T lymphocytes, respectively (Fig. 3g, h). In contrast, 3BNC117 alone, to which our SHIV-SF162P3 stock was relatively resistant, resulted in only a transient 0.2–1.1 log reduction of plasma viral loads (Fig. 3b), and one animal in this group (monkey CW9G) was euthanized for progressive clinical AIDS during this experiment.

## Kinetics of virologic control

The kinetics of the initial decline of plasma viremia following infusion of PGT121 or PGT121-containing mAb cocktails was a median of 0.382 logs/day (IQR 0.338–0.540). In contrast, the initial kinetics of decline of plasma viremia following raltegravir-containing combination antiretroviral therapy in HIV-1-infected humans was a median of 0.264 logs/day (IQR 0.253–0.284)[28] and following combination antiretroviral therapy in SIV-infected monkeys was a median of 0.229 logs/day (IQR 0.198–0.265) (J.B.W., unpublished data) (Extended Data Table 1). Although these reflect different models, the rapid control of virus following mAb administration is striking and consistent with a mechanism that involves direct elimination of free virus in plasma in addition to virus-infected cells in tissues. The rapid reduction of proviral DNA in PBMC by day 1 (Fig. 1e) suggests direct

antibody-mediated cytotoxic effects on infected cells[29], although we cannot exclude the possibility of an effect of CD4+ T cell trafficking.

## Summary and implications

Our studies demonstrate the therapeutic efficacy of PGT121 and PGT121-containing mAb cocktails in chronically SHIV-SF162P3 infected rhesus monkeys. The therapeutic efficacy in the 18 animals that received PGT121 alone or as part of a cocktail (Fig. 4a) was dependent on baseline viral loads before mAb administration. In the 17% of animals (3 of 18) with low baseline viral loads <3.5 log RNA copies/ml, long-term control of viral replication was observed for the duration of the follow-up period (Fig. 4b), which included a substantial period of time after serum mAb titers had declined to undetectable levels. These observations suggest that PGT121 may have converted animals with low baseline viremia into “elite controllers”, although additional follow-up is required to assess the durability of this effect. These animals still have detectable, albeit reduced, proviral DNA in tissues (Fig. 2g, h; Fig. 3e, f), and thus virus has not been eradicated in these animals. In the 72% of animals (13 of 18) with intermediate baseline viral loads 3.5–5.3 log RNA copies/ml, plasma viremia was rapidly reduced to undetectable levels within 7 days but then rebounded in a median of 56 days when serum mAb titers declined to undetectable levels <1 μg/ml (Fig. 4c). In the 11% of animals (2 of 18) with high baseline viral loads >5.3 log RNA copies/ml, incomplete control of plasma viremia and rapid viral rebound was observed, suggesting a therapeutic ceiling in this model (Fig. 4d). Taken together, baseline viral loads strongly correlated with the time to viral rebound (P=0.0002, Spearman rank-correlation test; Fig. 4e).

We speculate that the therapeutic impact of these mAbs reflected not only their direct antiviral activity but also their impact on host antiviral immune responses. Following mAb infusion, we observed modest increases in host virus-specific NAb activity (Extended Data Fig. 2) as well as reduced activation and improved functionality of host virus-specific T lymphocyte responses (Fig. 1f–h; Fig. 2e, f; Fig. 3g, h). Consistent with this model, median log setpoint viral loads following viral rebound were 0.61 log lower than median setpoint viral loads at baseline prior to mAb infusion (P=0.0005, Wilcoxon matched pairs signed-rank test; Fig. 4f), with no evidence of reduced viral replicative capacity[30] (Extended Data Fig. 8). Moreover, 3 of 18 monkeys exhibited persistent virologic control to undetectable levels (Fig. 4b). Defining the precise immunologic mechanisms of improved virologic control following monoclonal and polyclonal antibody administration[31,32] warrants further investigation.

Previous studies in humanized mice and humans showed that the earlier generation of neutralizing HIV-1-specific mAbs was unable to control viremia[15–17]. More recent studies in humanized mice have shown that combinations of 3 or 5 of the new generation of more potent mAbs suppressed HIV-1 replication, although single mAbs still rapidly selected for resistance[18,19]. In contrast to these prior studies, we observed that a single infusion of PGT121 in rhesus monkeys resulted in rapid virologic control in both peripheral blood and tissues. It is possible that intrinsic differences between HIV-1 replication in mice and SHIV replication in monkeys may account for these differences. Another key difference is the

functional immune system in rhesus monkeys as compared with immunosuppressed humanized mice, and the profound virologic suppression without the development of resistance in the present study may reflect functional host antibody effector activity and intact antiviral cellular immune responses in rhesus monkeys. A caveat is that we were unable to quantitate the intrinsic ability of SHIV-SF162P3 to escape from PGT121 *in vivo*, although prior studies have documented the ability of SHIV-SF162P3 and SHIV-SF162P4 to escape from autologous antibody responses in other settings[33,34]. Moreover, N332A-mutated SHIV-SF162P3 exhibited only partial escape from PGT121 *in vitro* but complete escape from other N332-dependent mAbs PGT124 and PGT128, suggesting a high bar to resistance (Extended Data Fig. 9).

## Conclusions

Our data demonstrate profound therapeutic efficacy of broad and potent HIV-1-specific mAbs in rhesus monkeys chronically infected with SHIV-SF162P3. Our SHIV-SF162P3 stock is highly pathogenic, as evidenced by moderate to high chronic setpoint viral loads and AIDS-related deaths in two animals during the course of these experiments (Figs. 2c, 3b). Moreover, in a separate study[35], our SHIV-SF162P3 stock led to AIDS-related mortality in 5 of 12 (42%) rhesus monkeys by 1 year following infection, which is comparable to the reported pathogenicity of SIVmac251[36,37] and SHIV-AD8[38,39]. Nevertheless, given the differences between SHIV-infected rhesus monkeys and HIV-1-infected humans, clinical trials are required to establish the therapeutic efficacy of potent neutralizing HIV-1-specific mAbs in humans. Although multiple mAbs targeting different epitopes will likely prove superior, our data suggest that mAb monotherapy with the new generation of potent and broad mAbs also warrants clinical evaluation. Moreover, the ability of these mAbs to reduce proviral DNA in tissues suggests that these mAbs should also be evaluated in the context of viral eradication strategies.

## Methods

### Animals and study design

34 Indian-origin, outbred, young adult, male and female, specific pathogen-free (SPF) rhesus monkeys (*Macaca mulatta*) that did not express the class I alleles *Mamu-A*01*, *Mamu-B*08*, and *Mamu-B*17* associated with spontaneous virologic control were housed at New England Primate Research Center, Bioqual, or Alphagenesis. Groups were balanced for susceptible and resistant TRIM5α alleles. Groups of 4–5 monkeys were powered to detect large differences in viral loads, and animals were randomly allocated to balance baseline viral loads. Animals were infected by the intrarectal route with our rhesus-derived SHIV-SF162P3 challenge stock for 9 months prior to mAb administration were utilized for the studies. PGT121, b12, and DEN3 mAbs were generated as previously described[10] and were expressed in Chinese hamster ovary (CHO-K1) cells and purified by Protein A affinity chromatography. 3BNC117 was manufactured by Celldex Therapeutics in CHO cells and purified by chromatography and sterile filtration. All the mAb preparations were endotoxin free. Cocktails of mAbs or single mAbs were administered to monkeys once or twice by the intravenous route at a dose of 10 mg/kg for each mAb. Monkeys were bled up to three times

per week for viral loads. Immunologic and virologic data were generated blinded. All animal studies were approved by the appropriate Institutional Animal Care and Use Committee (IACUC).

### Cellular immune assays

SIV Gag-specific cellular immune responses were assessed by multiparameter intracellular cytokine staining (ICS) assays essentially as described[23,24]. 12-color ICS assays were performed with the Aqua green-fluorescent reactive dye (Invitrogen, L23101) and predetermined titers of mAbs (Becton-Dickinson) against CD3 (SP34; Alexa Fluor 700), CD4 (OKT4; BV711, Biolegend), CD8 (SK1; allophycocyanin-cyanine 7 [APC-Cy7]), CD28 (L293; BV610), CD95 (DX2; allophycocyanin [APC]), CD69 (TP1.55.3; phycoerythrin-Texas red [energy-coupled dye; ECD]; Beckman Coulter), gamma interferon (IFN-$\gamma$) (B27; phycoerythrin-cyanine 7 [PE-Cy7]), Ki67 (B56; fluorescein isothiocyanate [FITC]), CCR5 (3A9; phycoerythrin [PE]), CCR7(3D12; Pacific Blue), and PD-1(EH21.1; peridinin chlorophyll-A-cyanine 5.5 [PerCP-Cy5.5]). IFN-$\gamma$ backgrounds were consistently <0.01% in PBMC and LNMC and <0.05% in colorectal biopsy specimens. Virus suppression assays (VSA) were performed by co-culturing purified CD8+ T lymphocytes with CD8-depleted PBMC and monitoring p27 levels for 7–14 days essentially as described[25].

### Neutralizing antibody assays

HIV-1-specific neutralizing antibody (NAb) responses against primary infectious stocks of SHIV-SF162P3 and SHIV-SF162P4 were assessed by TZM-bl luciferase-based neutralization assays[22]. PGT121 titers were determined by X2088_c9 and ZM247v1(Rev-) pseudovirus neutralization, 3BNC117 titers were determined by 6041.v3.c23 and Q461.ez pseudovirus neutralization, and b12 titers were determined by Du422.1.N332A pseudovirus neutralization and B2.1 ELISA.

### Proviral DNA assay

Proviral DNA was quantitated as previously reported[26]. Lymph node and gastrointestinal mucosal biopsies were processed as single cell suspensions essentially as previously described[27]. Tissue-specific total cellular DNA was isolated from $5\times10^6$ cells using a QIAamp DNA Blood Mini kit (Qiagen). The absolute quantification of viral DNA in each sample was determined by qPCR using primers specific to a conserved region SIVmac239. All samples were directly compared to a linear virus standard and the simultaneous amplification of a fragment of human GAPDH gene. The sensitivity of linear standards was compared against the 3D8 cell line as a reference standard as described[26]. All PCR assays were performed with 100 and 200 ng of sample DNA.

### Virus sequencing

Virus sequencing of breakthrough virus was performed essentially as described[18]. Plasma samples of 1 ml were centrifuged for 30 min at 20,000 × *g* and the lowest fraction was subjected to RNA purification (QiaAmp MinElute Virus Spin kit; Qiagen). Random hexamers (Roche) or SHIV-SF162P3-specific (5′-AAGAGCTCCTCCAGACAGTGAG-3′

or 5′-TAGAGCCCTGGAAGCATCCAGGAAGTCAGCCTA-3′) primers were used for cDNA synthesis with SuperScript™ III Reverse Transcriptase (Invitrogen). SHIV envelope sequences were amplified by a double–nested PCR approach using the Expand High Fidelity PCR System (Roche). First round primers for gp120 were 5′-AAGAGCTCCTCCAGACAGTGAG-3′ and 5′-ATGAGTTTTCCAGAGCAACCC-3′ and for gp160 were 5′-AAGAGCTCCTCCAGACAGTGAG-3′ and 5′-CAAGCCCTTGTCTAATCCTCC-3′. Second round primers for gp120 were 5′-GAAAGAGCAGAAGACAGTGGC-3′ and 5′-ATTGTCTGGCCTGTACCGTC-3′ and for gp160 were 5′-GAAAGAGCAGAAGACAGTGGC-3′ and 5′-ATGGAAATAGCTCCACCCATC-3′. Following second round PCR, all products were spiked with 0.5 μl *Taq* polymerase and incubated for 15 min at 72°C. Amplicons were excised from a gel and purified following cloning into the pCR™4-TOPO vector (Invitrogen) and expansion in One Shot® TOP10 cells at 30°C. Single colonies were sequenced using M13F/M13R primers as well as primers annealing to the envelope sequence. A consensus sequence of each clone was derived using Geneious Pro software (Biomatters), and sequence analysis was performed using Geneious Pro and antibody database software[21].

### Statistical analyses

Analyses of independent virologic and immunologic data were performed by two-tailed Mann-Whitney tests. Analyses of paired data sets were performed by two-tailed Wilcoxon matched pairs signed-rank tests. Correlations were evaluated by Spearman rank-correlation tests. P values less than 0.05 were considered significant. Statistical analyses were performed using GraphPad Prism. Exponential decay rates of plasma viral loads were calculated using standard ordinary least squares regression on $\log_{10}$ (viral load) measurements vs. time (days).

## Supplementary Material

Refer to Web version on PubMed Central for supplementary material.

## Acknowledgments

We thank A. Brinkman, M. Ferguson, C. Gittens, R. Geleziunas, R. Hamel, K. Kelly, J. Kramer, A. McNally, D. Montefiori, L. Nogueira, L. Parenteau, M. Pensiero, L. Peter, M. Shetty, D. Sok, K. Stanley, F. Stephens, W. Wagner, B. Walker, A. West, and J. Yalley-Ogunro for generous advice, assistance, and reagents. The SIVmac239 Gag peptide pool was obtained from the NIH AIDS Research and Reference Reagent Program. We acknowledge support from the National Institutes of Health (AI055332, AI060354, AI078526, AI084794, AI095985, AI096040, AI10063, AI100148, AI100663); the Bill and Melinda Gates Foundation (OPP1033091, OPP1033115, OPP1040741, OPP1040753); the Ragon Institute of MGH, MIT, and Harvard; the Lundbeck Foundation; and the Stavros Niarchos Foundation. M.C.N. is a Howard Hughes Medical Institute investigator.

## References

1. Burton DR, Poignard P, Stanfield RL, Wilson IA. Broadly neutralizing antibodies present new prospects to counter highly antigenically diverse viruses. Science. 2012; 337:183–186. [PubMed: 22798606]
2. Klein F, et al. Antibodies in HIV-1 vaccine development and therapy. Science. 2013; 341:1199–1204. [PubMed: 24031012]

3. Wu X, et al. Rational design of envelope identifies broadly neutralizing human monoclonal antibodies to HIV-1. Science. 2010; 329:856–861. [PubMed: 20616233]
4. Zhou T, et al. Structural basis for broad and potent neutralization of HIV-1 by antibody VRC01. Science. 2010; 329:811–817. [PubMed: 20616231]
5. Scheid JF, et al. Broad diversity of neutralizing antibodies isolated from memory B cells in HIV-infected individuals. Nature. 2009; 458:636–640. [PubMed: 19287373]
6. Scheid JF, et al. Sequence and structural convergence of broad and potent HIV antibodies that mimic CD4 binding. Science. 2011; 333:1633–1637. [PubMed: 21764753]
7. Diskin R, et al. Increasing the potency and breadth of an HIV antibody by using structure-based rational design. Science. 2011; 334:1289–1293. [PubMed: 22033520]
8. Walker LM, et al. Broad and potent neutralizing antibodies from an African donor reveal a new HIV-1 vaccine target. Science. 2009; 326:285–289. [PubMed: 19729618]
9. McLellan JS, et al. Structure of HIV-1 gp120 V1/V2 domain with broadly neutralizing antibody PG9. Nature. 2011; 480:336–343. [PubMed: 22113616]
10. Walker LM, et al. Broad neutralization coverage of HIV by multiple highly potent antibodies. Nature. 2011; 477:466–470. [PubMed: 21849977]
11. Julien JP, et al. Broadly neutralizing antibody PGT121 allosterically modulates CD4 binding via recognition of the HIV-1 gp120 V3 base and multiple surrounding glycans. PLoS Pathog. 2013; 9:e1003342. [PubMed: 23658524]
12. Mouquet H, et al. Complex-type N-glycan recognition by potent broadly neutralizing HIV antibodies. Proc Natl Acad Sci U S A. 2012; 109:E3268–3277. [PubMed: 23115339]
13. Kong L, et al. Supersite of immune vulnerability on the glycosylated face of HIV-1 envelope glycoprotein gp120. Nature structural & molecular biology. 2013; 20:796–803.
14. Huang J, et al. Broad and potent neutralization of HIV-1 by a gp41-specific human antibody. Nature. 2012; 491:406–412. [PubMed: 23151583]
15. Poignard P, et al. Neutralizing antibodies have limited effects on the control of established HIV-1 infection in vivo. Immunity. 1999; 10:431–438. [PubMed: 10229186]
16. Trkola A, et al. Delay of HIV-1 rebound after cessation of antiretroviral therapy through passive transfer of human neutralizing antibodies. Nat Med. 2005; 11:615–622. [PubMed: 15880120]
17. Mehandru S, et al. Adjunctive passive immunotherapy in human immunodeficiency virus type 1-infected individuals treated with antiviral therapy during acute and early infection. J Virol. 2007; 81:11016–11031. [PubMed: 17686878]
18. Klein F, et al. HIV therapy by a combination of broadly neutralizing antibodies in humanized mice. Nature. 2012; 492:118–122. [PubMed: 23103874]
19. Diskin R, et al. Restricting HIV-1 pathways for escape using rationally designed anti-HIV-1 antibodies. J Exp Med. 2013; 210:1235–1249. [PubMed: 23712429]
20. Burton DR, et al. Efficient neutralization of primary isolates of HIV-1 by a recombinant human monoclonal antibody. Science. 1994; 266:1024–1027. [PubMed: 7973652]
21. West AP Jr, et al. Computational analysis of anti-HIV-1 antibody neutralization panel data to identify potential functional epitope residues. Proc Natl Acad Sci U S A. 2013; 110:10598–10603. [PubMed: 23754383]
22. Montefiori, D. Evaluating neutralizing antibodies against HIV, SIV and SHIV in luciferase reporter gene assays. Current Protocols in Immunology. John Wiley & Sons; 2004.
23. Pitcher CJ, et al. Development and homeostasis of T cell memory in rhesus macaque. J Immunol. 2002; 168:29–43. [PubMed: 11751943]
24. Liu J, et al. Magnitude and phenotype of cellular immune responses elicited by recombinant adenovirus vectors and heterologous prime-boost regimens in rhesus monkeys. J Virol. 2008; 82:4844–4852. [PubMed: 18337575]
25. Stephenson KE, Li H, Walker BD, Michael NL, Barouch DH. Gag-specific cellular immunity determines in vitro viral inhibition and in vivo virologic control following simian immunodeficiency virus challenges of vaccinated rhesus monkeys. J Virol. 2012; 86:9583–9589. [PubMed: 22761379]

26. Whitney JB, et al. T-cell vaccination reduces simian immunodeficiency virus levels in semen. J Virol. 2009; 83:10840–10843. [PubMed: 19640980]
27. Li H, et al. Durable mucosal simian immunodeficiency virus-specific effector memory T lymphocyte responses elicited by recombinant adenovirus vectors in rhesus monkeys. J Virol. 2011; 85:11007–11015. [PubMed: 21917969]
28. Andrade A, et al. Three Distinct Phases of HIV-1 RNA Decay in Treatment-Naive Patients Receiving Raltegravir-Based Antiretroviral Therapy: ACTG A5248. J Infect Dis. 2013
29. Horwitz JA, et al. HIV-1 suppression and durable control by combining single broadly neutralizing antibodies and antiretroviral drugs in humanized mice. Proc Natl Acad Sci U S A. 2013
30. Cornall A, et al. A novel, rapid method to detect infectious HIV-1 from plasma of persons infected with HIV-1. Journal of virological methods. 2010; 165:90–96. [PubMed: 20117138]
31. Jaworski JP, et al. Neutralizing Polyclonal IgG Present during Acute Infection Prevents Rapid Disease Onset in Simian-Human Immunodeficiency Virus SHIVSF162P3-Infected Infant Rhesus Macaques. J Virol. 2013; 87:10447–10459. [PubMed: 23885083]
32. Ng CT, et al. Passive neutralizing antibody controls SHIV viremia and enhances B cell responses in infant macaques. Nat Med. 2010; 16:1117–1119. [PubMed: 20890292]
33. Jayaraman P, et al. Evidence for persistent, occult infection in neonatal macaques following perinatal transmission of simian-human immunodeficiency virus SF162P3. J Virol. 2007; 81:822–834. [PubMed: 17079310]
34. Kraft Z, et al. Macaques infected with a CCR5-tropic simian/human immunodeficiency virus (SHIV) develop broadly reactive anti-HIV neutralizing antibodies. J Virol. 2007; 81:6402–6411. [PubMed: 17392364]
35. Barouch DH. Protective efficacy of a global HIV-1 mosaic vaccine against heterologous SHIV challenges in rhesus monkeys. Cell. 2013 in press.
36. Barouch DH, et al. Vaccine protection against acquisition of neutralization-resistant SIV challenges in rhesus monkeys. Nature. 2012; 482:89–93. [PubMed: 22217938]
37. Liu J, et al. Immune control of an SIV challenge by a T-cell-based vaccine in rhesus monkeys. Nature. 2009; 457:87–91. [PubMed: 18997770]
38. Nishimura Y, et al. Generation of the pathogenic R5-tropic simian/human immunodeficiency virus SHIVAD8 by serial passaging in rhesus macaques. J Virol. 2010; 84:4769–4781. [PubMed: 20147396]
39. Gautam R, et al. Pathogenicity and mucosal transmissibility of the R5-tropic simian/human immunodeficiency virus SHIV(AD8) in rhesus macaques: implications for use in vaccine studies. J Virol. 2012; 86:8516–8526. [PubMed: 22647691]

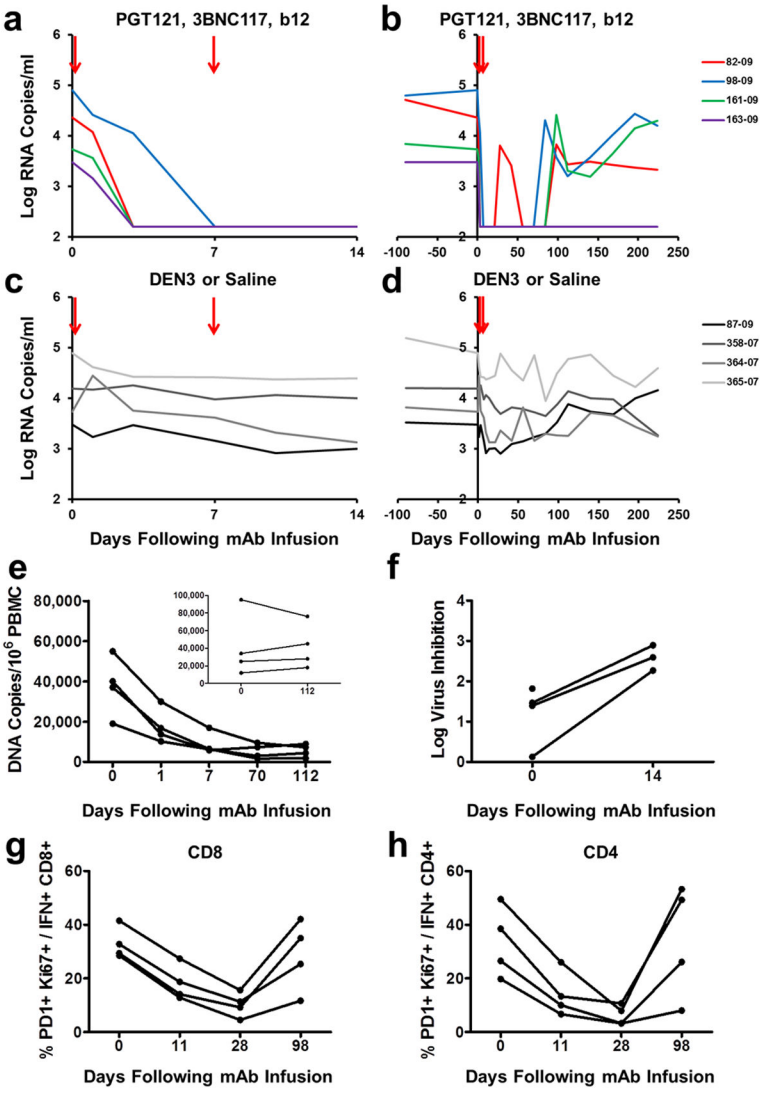


**Figure 1. Therapeutic efficacy of the triple PGT121/3BNC117/b12 mAb cocktail**

Plasma viral RNA (log copies/ml) in rhesus monkeys chronically infected with SHIV-SF162P3 following infusions of PGT121, 3BCN117, and b12 on day 0 and day 7 (arrows) for 14 days (**a**) and 224 days (**b**). Plasma viral RNA in rhesus monkeys chronically infected with SHIV-SF162P3 following infusions with the control mAb DEN3 (87-09) or saline on day 0 and day 7 (arrows) for 14 days (**c**) and 224 days (**d**). **e**, Proviral DNA (copies/$10^6$ PBMC) in the monkeys that received the therapeutic mAb cocktail or controls (inset). **f**, Log inhibition of viral replication in CD8+ T lymphocyte virus suppression assays following mAb infusion. One animal had no recoverable virus at week 2. PD-1+Ki67+ expression on Gag-specific CD8+ (**g**) and CD4+ (**h**) T lymphocytes following mAb infusion.

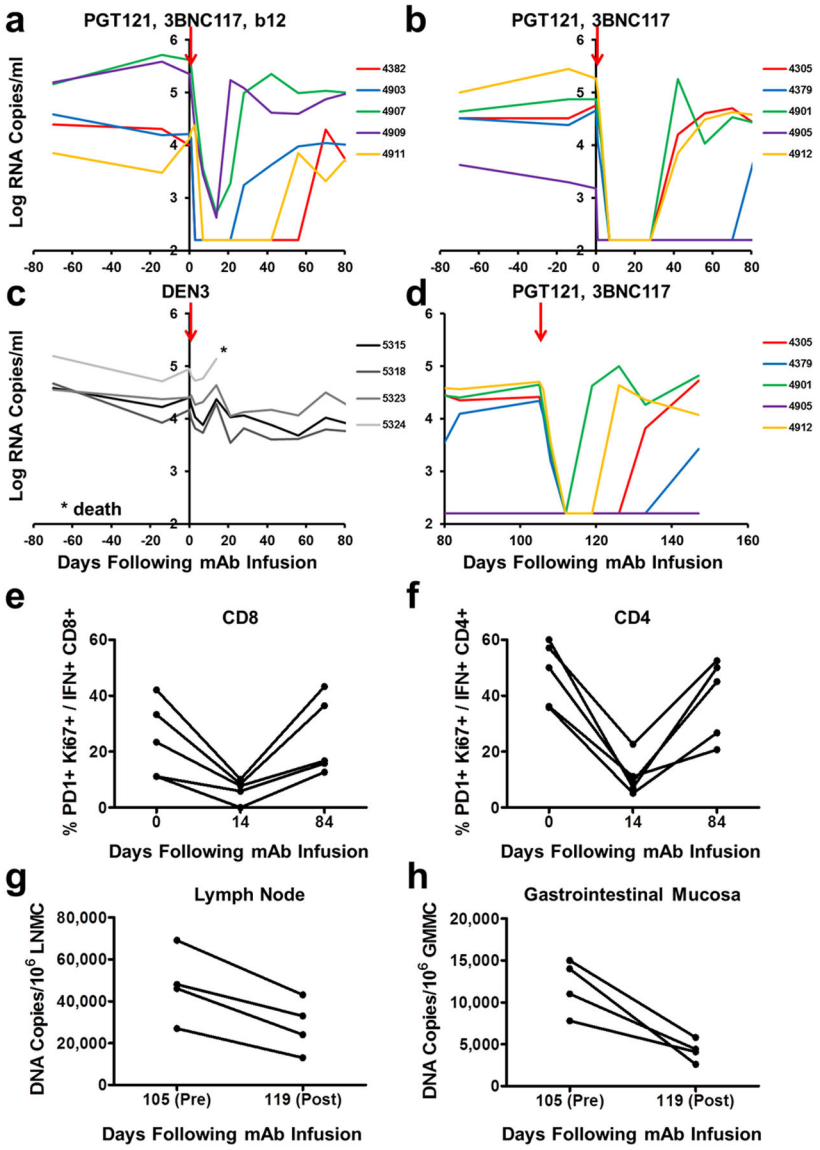


**Figure 2. Therapeutic efficacy of the double PGT121/3BNC117 mAb cocktail**

Plasma viral RNA (log copies/ml) in rhesus monkeys chronically infected with SHIV-SF162P3 following a single infusion (arrows) of PGT121, 3BCN117, and b12 (**a**); PGT121 and 3BNC117 (**b**); or the control mAb DEN3 (**c**). **d**, Plasma viral RNA in monkeys that received PGT121 and 3BNC117 following a second infusion on day 105. PD-1+Ki67+ expression on Gag-specific CD8+ (**e**) and CD4+ (**f**) T lymphocytes in the monkeys that received PGT121 and 3BNC117. Proviral DNA (copies/$10^6$ cells) in lymph nodes (**g**) and gastrointestinal mucosa (**h**) before (day 105) and 14 days after (day 119) the second mAb infusion with PGT121 and 3BNC117 in the four animals with detectable viremia.

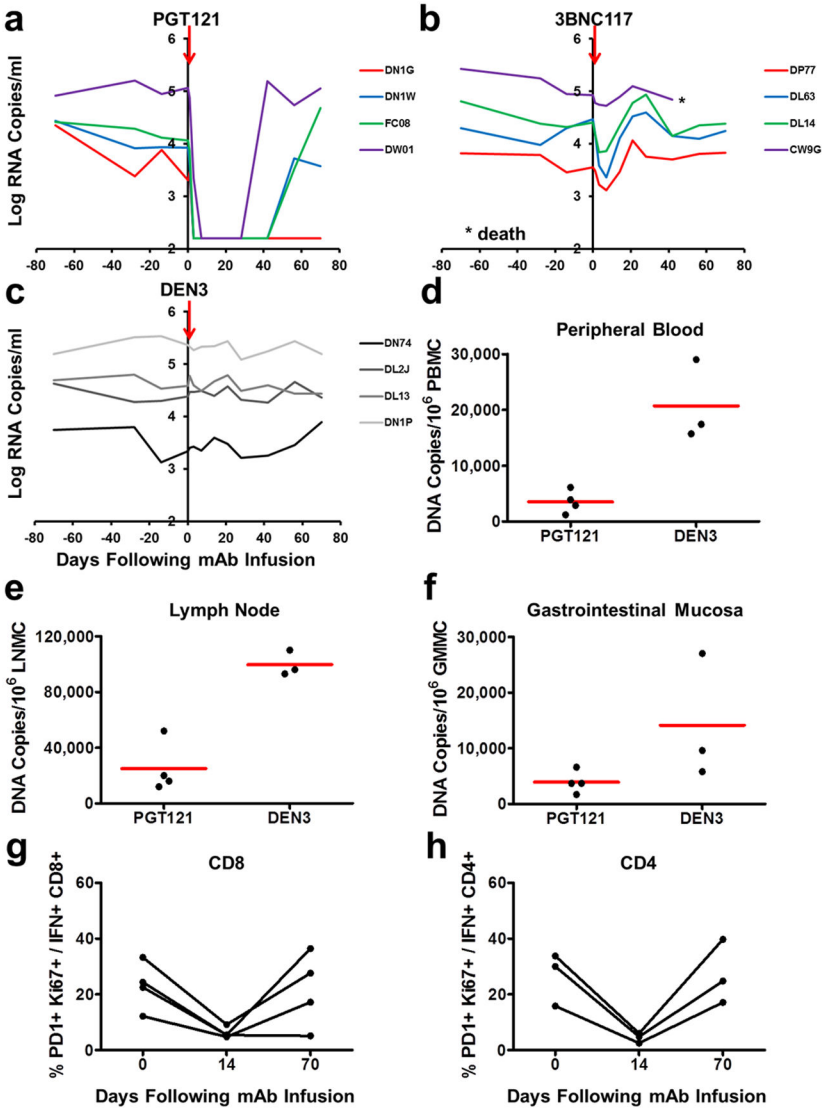


**Figure 3. Therapeutic efficacy of the single mAbs PGT121 and 3BNC117**

Plasma viral RNA (log copies/ml) in rhesus monkeys chronically infected with SHIV-SF162P3 following a single infusion (arrows) of PGT121 (**a**), 3BNC117 (**b**), or the control mAb DEN3 (**c**). Proviral DNA (copies/$10^6$ cells) in PBMC (**d**), lymph nodes (**e**), and gastrointestinal mucosa (**f**) 14 days following the mAb infusion in the animals that received PGT121 or DEN3. Red bars indicate means. Assays for one of the DEN3 treated controls failed. PD-1+Ki67+ expression on Gag-specific CD8+ (**g**) and CD4+ (**h**) T lymphocytes in the monkeys that received PGT121.

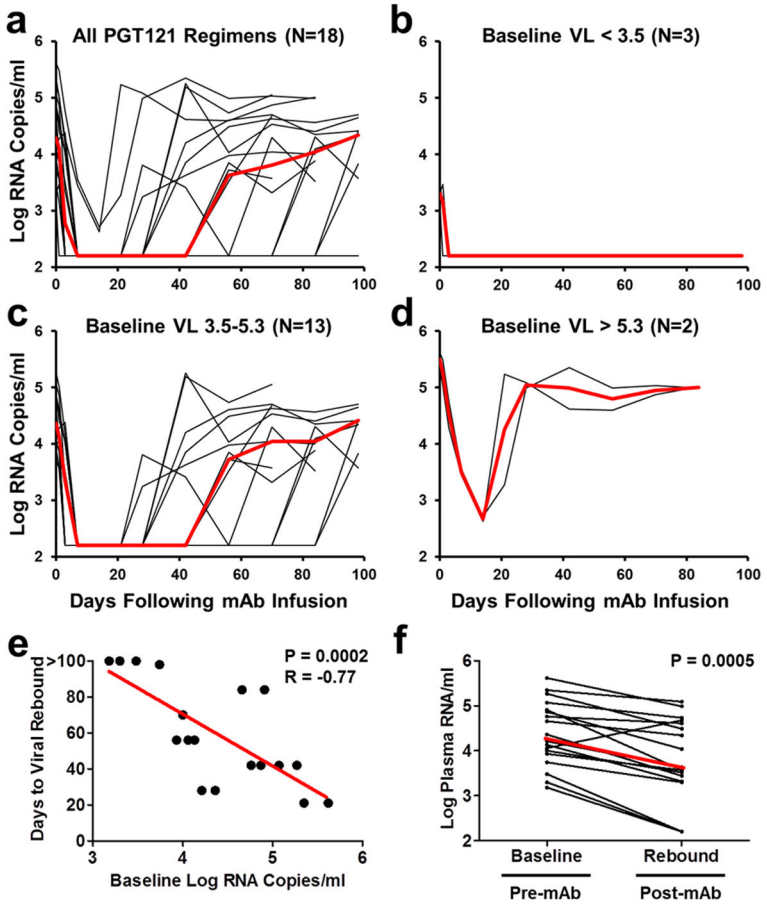


**Figure 4. Therapeutic efficacy of PGT121 or PGT121-containing mAb cocktails in chronically SHIV-infected rhesus monkeys**

**a**, Summary of the therapeutic effect of PGT121 alone or PGT121-containing mAb cocktails in the 18 rhesus monkeys chronically infected with SHIV-SF162P3, as well as in the subgroups of animals with baseline viral loads of <3.5 log RNA copies/ml (N=3) (**b**), 3.5–5.3 log RNA copies/ml (N=13) (**c**), and >5.3 log RNA copies/ml (N=2) (**d**). Red lines indicates median log viral loads. **e**, Correlation of baseline viral loads with times to viral rebound. P value reflects two-sided Spearman rank-correlation test. **f**, Comparison of setpoint viral loads at baseline before mAb administration and following viral rebound. P value reflects two-sided Wilcoxon matched pairs signed-rank test. Red line indicates median log viral loads.

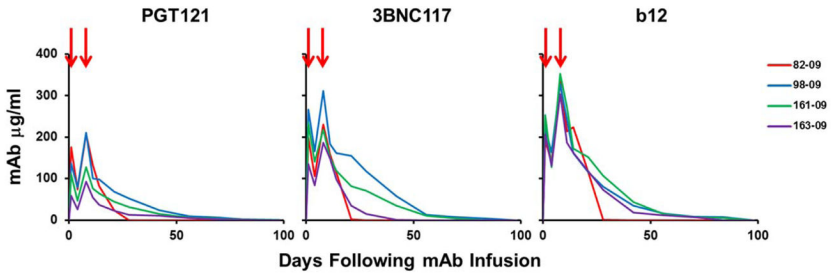


**Extended Data Figure 1. Monoclonal Ab titers following administration of the triple PGT121/3BNC117/b12 mAb cocktail**

PGT121, 3BNC117, and b12 titers in the monkeys described in Fig. 1 following infusion of the triple mAb cocktail (arrows).

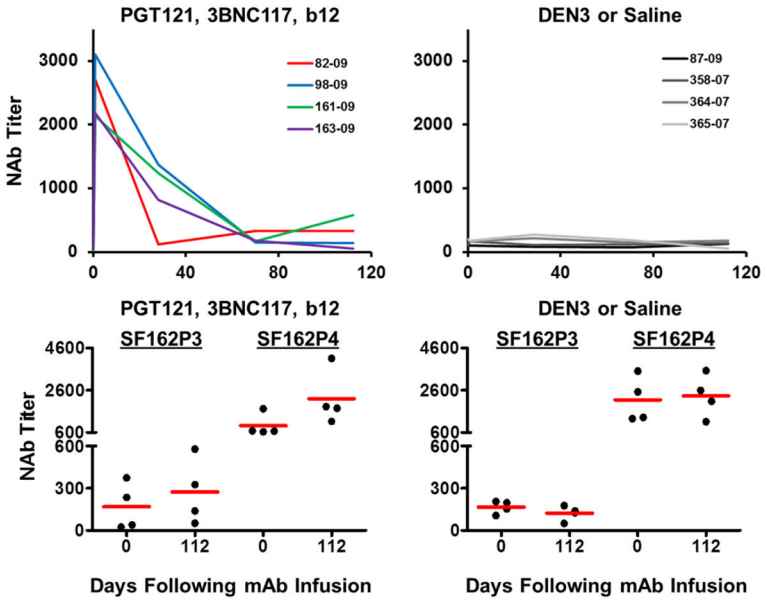


**Extended Data Figure 2. Neutralizing Ab titers following administration of the triple PGT121/3BNC117/b12 mAb cocktail**

SHIV-SF162P3 and SHIV-SF162P4 serum NAb ID50 titers in the monkeys described in Fig. 1 following infusion of the triple mAb cocktail (left) or saline or DEN3 (right).

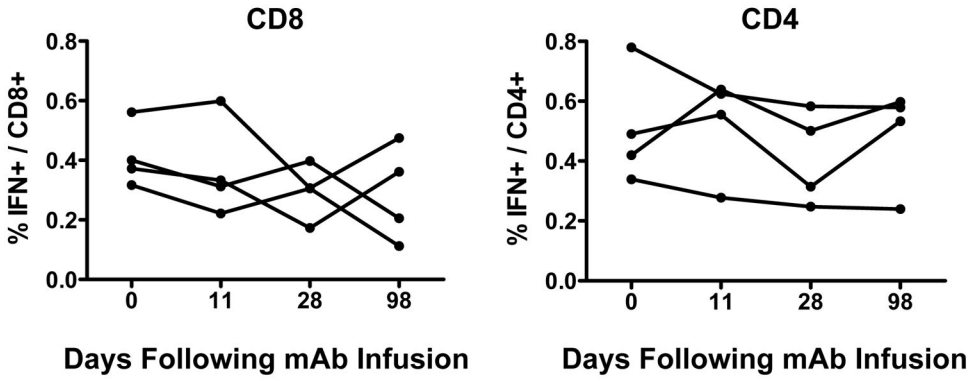


**Extended Data Figure 3. Gag-specific T lymphocyte responses following administration of the triple PGT121/3BNC117/b12 mAb cocktail**

Gag-specific IFN-γ+ CD8+ (left) and CD4+ (right) T lymphocyte responses in the monkeys described in Fig. 1 following infusion of the triple mAb cocktail.

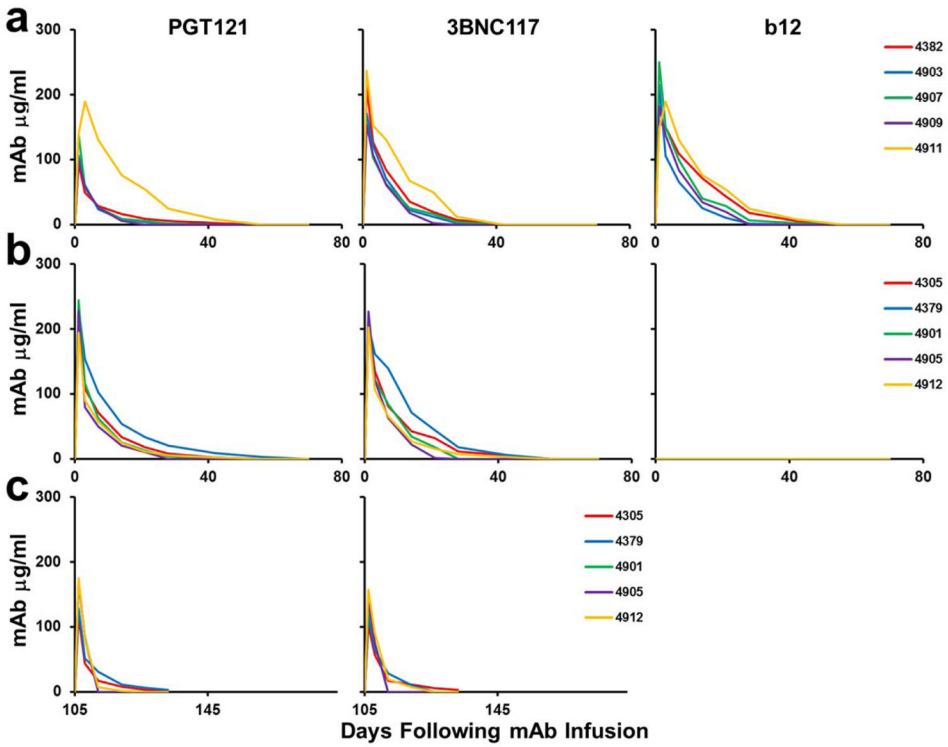


**Extended Data Figure 4. Monoclonal Ab titers following administration of the double PGT121/3BNC117 mAb cocktail**

PGT121, 3BNC117, and b12 titers in the monkeys described in Fig. 2 that received PGT121, 3BCN117, and b12 (**a**); PGT121 and 3BNC117 (**b**); or the second infusion of PGT121 and 3BNC117 (**c**).

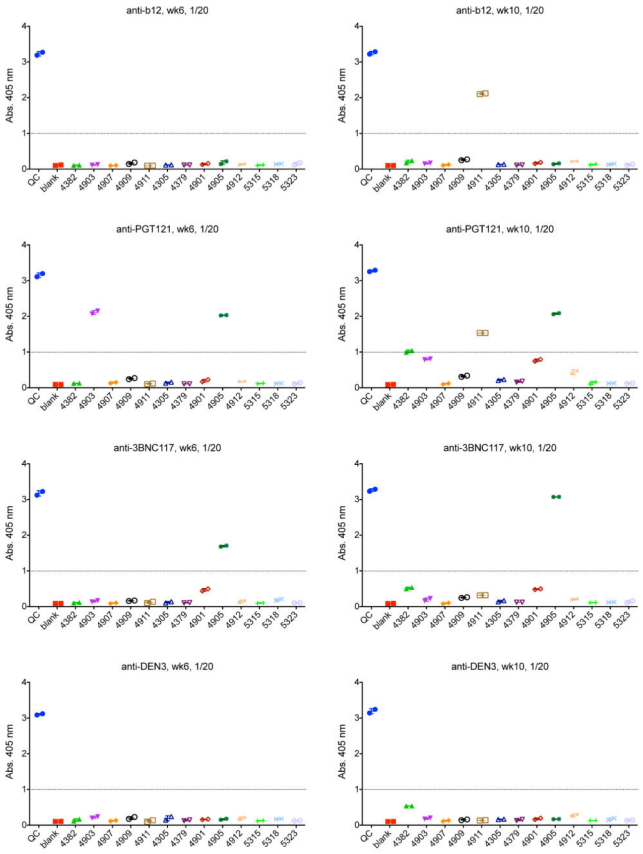


**Extended Data Figure 5. Monkey anti-human antibody titers following mAb administration**

ELISAs assessing anti-b12, anti-PGT121, anti-3BNC117, and anti-DEN3 antibodies at week 6 and week 10 following mAb infusion in the monkeys described in Fig. 2.

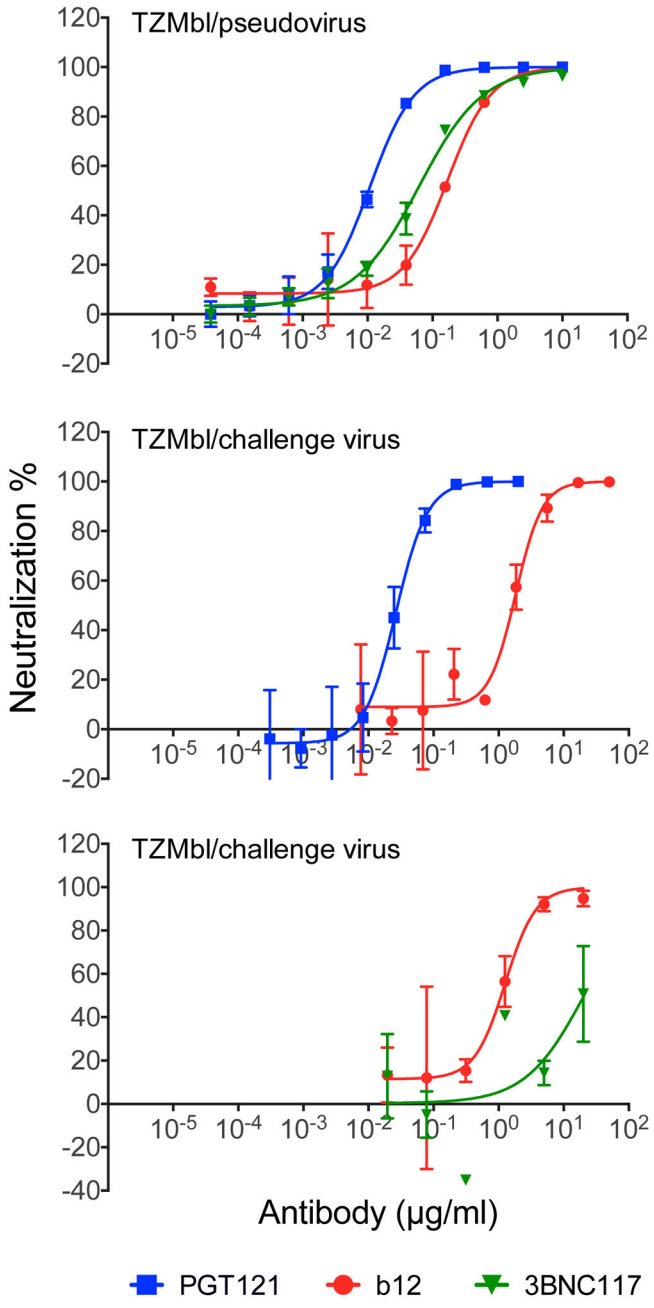


**Extended Data Figure 6. Neutralization sensitivity of SHIV-SF162P3 pseudovirus and our SHIV-SF162P3 challenge stock**

TZM-bl neutralization assays of PGT121, 3BNC117, and b12 against the SHIV-SF162P3 pseudovirus (top) and against the SHIV-SF162P3 challenge stock (middle, bottom). Note sensitivity of our SHIV-SF162P3 challenge stock to PGT121 but relative resistance to 3BNC117.

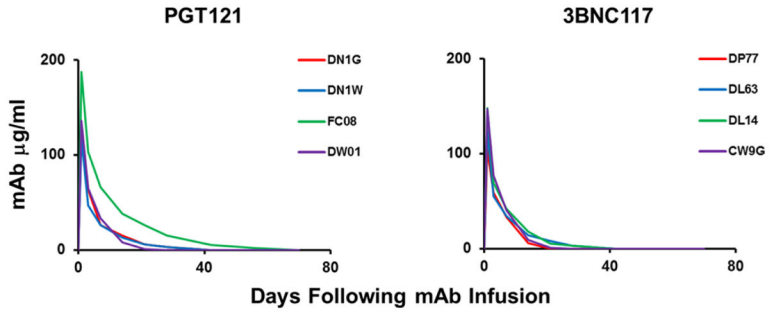


**Extended Data Figure 7. Monoclonal Ab titers following administration of the single mAbs PGT121 and 3BNC117**

PGT121 and 3BNC117 titers in the monkeys described in Fig. 3 following infusion of the single mAbs.

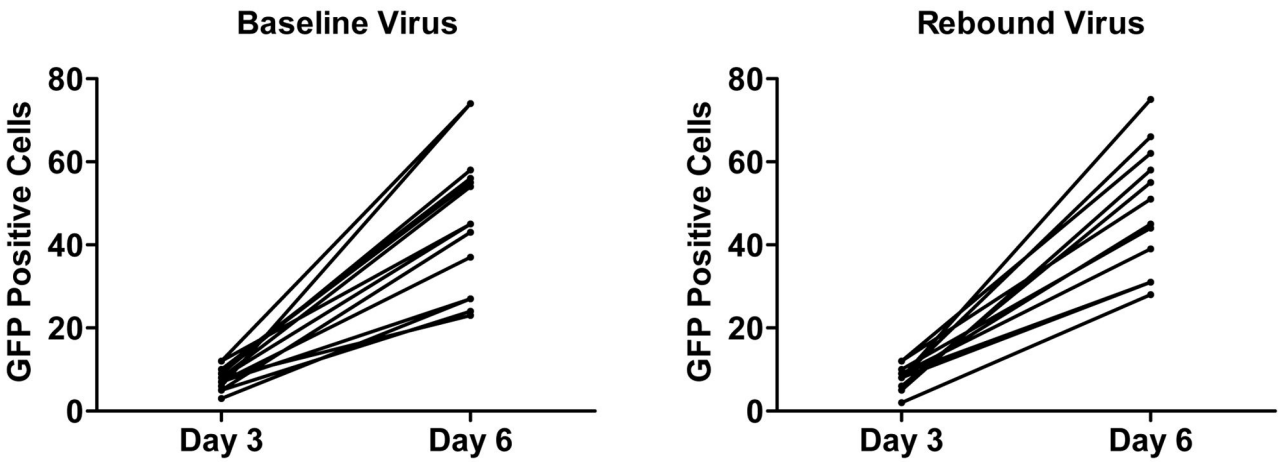


**Extended Data Figure 8. Virus replicative capacity and following virus rebound**

Numbers of GFP positive infected GHOST indicator cells per well after 3 and 6 days of culture with baseline or rebound SHIV-SF162P3 virus.

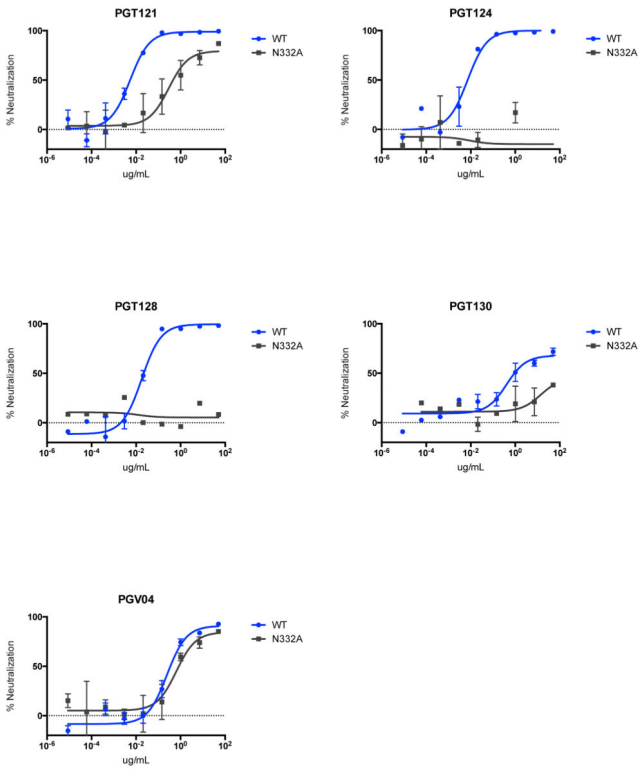


**Extended Data Figure 9. Monoconal antibody sensitivity to N332A mutated SHIV-SF162P3**

TZM-bl neutralization assays of PGT121, PGT124, PGT128, PGT130, and PGV04 against SHIV-SF162P3 containing the N332A mutation. Note 100-fold reduced sensitivity to PGT121 but more profound escape from PGT124 and PGT128.

## Extended Data Table 1

Viral decay kinetics.Kinetics of decline of plasma viremia following antiretroviral therapy in rhesus monkeys and humans and following mAb administration in rhesus monkeys.

| Therapy | *r* (logs/day)[†] Median (IQR) | Median $t_{1/2}$ (days)[#] | Fold decrease in viral load over a 7-day period |
|---|---|---|---|
| DTG + TNF/FTC (SIV/monkeys) | 0.229 (0.198–0.265)[*] | 1.31 | 40 |
| EFV + 2 NRTI (HIV/humans) | 0.294 (0.273–0.334) | 1.02 | 112 |
| RAL + TDF/FTC (HIV/humans) | 0.264 (0.253–0.284) | 1.15 | 70 |
| PGT121 mAb (SHIV/monkeys) | 0.382 (0.338–0.540) | 0.78 | 468 |

[†] In case of EFV and RAL therapies, decline rates *r* correspond to the "first phase" of viral decline. Values reported in ref. 23 have been converted to logs/day (base 10). Note that the specific rate of decline due to RAL is slower than that due to EFV. The rapid viral decline in RAL compared to EFV is due to a longer duration in the first phase and a slower transition into the second phase, where viral decline rates are lower.

[#] The half-life, $t_{1/2} = \ln(2)/r*\ln(10)$.

[*] Computed using viral load measurements at day 0 and day 12 (J. B. W., unpublished).